Geophys. J. Int. (2003) **153,** 75–87

High-resolution body wave tomography beneath the SVEKALAPKO array: I. *A priori* three-dimensional crustal model and associated traveltime effects on teleseismic wave fronts

Senén Sandoval, Edi Kissling, Jörg Ansorge and the SVEKALAPKO Seismic Tomography Working Group

Institute of Geophysics, ETH Zurich, Switzerland. E-mail: senen@tomo.ig.erdw.ethz.ch

Accepted 2002 October 9. Received 2002 October 3; in original form 2001 September 20

SUMMARY

Assessment of contributions from shallow lithosphere to teleseismic wave front distortion is a prerequisite for high-resolution regional teleseismic tomography. Several methods have been proposed in the past for the correction of these effects, e.g. application of station correction terms. We propose an approach that is independent of the subsequent inversion and uses the available *a priori* knowledge of the crustal structure to calculate crustal traveltime effects of teleseismic wave fronts. Our approach involves the construction of a 3-D crustal model based on controlled source seismology data and calculation of the associated traveltime anomalies for incoming teleseismic wave fronts. The model for central Fennoscandia shows a maximum crustal thickness of 64 km and includes a high-velocity lower crust as derived for parts of the study area by previous authors. Traveltimes calculated using finite differences for teleseismic waves travelling through this crustal model are compared with those from the standard reference model IASP91 and the residuals are used to correct observed teleseismic arrival times at the SVEKALAPKO array. To test the performance of this approach, in a second part of the study a synthetic traveltime data set is obtained by tracing wave fronts through a mantle structure with known velocity anomalies and the 3-D crustal model. This data set is inverted with and without correction for crustal effects. The 3-D crustal effects alone with a homogeneous mantle are also inverted and the results show that the crustal effects propagate down to 450 km. The comparison of the inversion results demonstrates the need to apply appropriate 3-D crustal corrections in high-resolution regional tomography for upper-mantle structure beneath the Baltic Shield.

Key words: Baltic Shield, crustal structure, high-resolution teleseismic tomography.

1 INTRODUCTION

There have been significant advances in the theory and applications of seismic tomography since the pioneering work of Aki *et al.* (1977) (ACH method hereafter). These include refinements in model parametrization, 3-D ray tracing, inversion algorithms, resolution and error analyses, joint use of local, regional and teleseismic data, and the addition of converted and reflected waves in the tomographic inversion. Some of these problems and necessary modifications to the ACH method were discussed by Evans & Achauer (1993). More recently, Masson & Trampert (1997) found that the relative residuals generated outside the target volume might not be negligible. Julian *et al.* (2000) documented geometrical errors produced when azimuths on the spherical Earth are not properly transferred to the local coordinate system. A review of recent advances in 3-D ray-tracing methods may be found in Thurber & Kissling (2000) and for teleseismic 3-D ray tracing, in particular, we refer to Bijwaard *et al.* (1998). Consistency of phase identification of first and secondary arrivals also plays a major role in recent developments of global seismic tomography (e.g. Engdahl *et al.* 1998; Rohm *et al.* 2000). The single most important addition to the original ACH method regards the correction for shallow Earth structure.

High-resolution teleseismic tomography of the lithosphere–asthenosphere system requires appropriate crustal corrections because of strong wave scattering at crustal interfaces. If this adjustment is neglected, crustal effects are back-projected during the inversion and lead to artefacts in the derived structure of the underlying upper mantle. In the past, several methods have been proposed in order to overcome these difficulties. The first attempts to correct for shallow structure consisted of applying static terms (or corrections) to each individual station (Dziewonski & Anderson 1983). VandeCar *et al.* (1995) inverted simultaneously for the slowness perturbation field, earthquake relocations and station corrections. According to these authors, the station corrections are necessary to account for shallow crustal heterogeneities and differences in station elevations. The main drawback of this method is that the resolution

of teleseismic rays for shallow structure is very poor, resulting in significant vertical leakage. Takauchi & Evans (1995) tackled the problem from a different point of view. They addressed the problem of shallow vertical smearing by trying to back-project most of the observed anomalies into the shallowest layer and using the resulting velocity field as the top layer of the initial model for the subsequent 3-D inversion. The drawback of this approach is an overestimation of the crustal effect caused by vertical leakage of the uppermost mantle structure.

In addition, all the aforementioned methods are highly dependent on the inversion parameters (station and receiver distribution, damping, parametrization, etc.) and the results may not be compared with *a priori* known crustal structure. Therefore, we will follow the approach derived by Waldhauser *et al.* (1998) and Arlitt *et al.* (1999), which is independent of the subsequent inversion and makes use of *a priori* knowledge of crustal structure to calculate crustal effects on traveltimes of teleseismic wave fronts.

Seismic refraction, near-vertical and wide-angle reflection experiments are the most widely used, the most reliable and the most accurate seismic techniques in mapping the Earth's shallow structure. The first active source experiments took place during the early 1950s (e.g. Gutenberg 1959; Giese *et al.* 1976). Since then, extensive developments in data acquisition, processing and modelling techniques have led to the high spatial resolution of modern controlled source seismology (CSS) experiments and to more accurate geological and tectonic interpretations (e.g. Blundell *et al.* 1992). These well-documented laterally varying crustal structures, e.g. sedimentary basins, topography of the crust–mantle boundary (Moho) and average layer velocities can severely distort teleseismic wave fronts. Differences in teleseismic traveltime of between 1 and 2 s (Waldhauser *et al.* 1998; Arlitt *et al.* 1999) can be produced as a result of crustal structure variations.

In this paper we present a 3-D crustal model for central Fennoscandia based on CSS data. In a second step crustal traveltimes for teleseismic sources are calculated using 3-D ray tracing through our crustal model. The calculated traveltimes are compared with those from the 1-D standard reference model, IASP91 (Kennett & Engdahl 1991). The spatially varying differences in traveltime documents the distortion of the wave fronts owing to the 3-D crustal model, and they are used to correct the observed teleseismic traveltimes before tomographic inversion for mantle structure.

Finally, we check and demonstrate the significance of appropriate crustal corrections in high-resolution upper-mantle tomography with a synthetic data test. A synthetic traveltime data set calculated for a known mantle structure and for the derived 3-D crustal model is inverted twice, with and without the application of crustal corrections. Comparisons of these inversion results demonstrate the need to apply appropriate 3-D crustal corrections in high-resolution regional tomography for upper-mantle structure beneath the Baltic Shield. A second paper (Sandoval *et al.*, submitted) will focus on the investigation of the upper-mantle structure down to 400 km depth under central Fennoscandia (Baltic Shield) by applying the methodology described here to the SVEKALAPKO teleseismic data set.

2 THE SVEKALAPKO PROJECT

The Baltic Shield is one of the best preserved Precambrian cratons around the world and is the target of the multidisciplinary SVEKALAPKO experiment (Gee & Zeyen 1996; Bock *et al.* 2001). From a seismological point of view, this area presents optimal conditions (absence of sedimentary cover, small degree of alteration and a low population density or other sources of noise) to study in detail the structure of very old continental lithosphere and the mantle below by different geophysical methods. CSS studies show that the crustal thickness increases from 40 km in the Baltic Shield to over 60 km beneath central Finland, which has to be taken into account in all studies.

The SVEKALAPKO seismic study area extends from 59° to 68°N and 18° to 34°E (Fig. 1). For this large region, a network of temporary stations was designed with a total of 143 sensors including 15 permanent stations. The network comprised 40 broad-band and 88 short-period stations. The array was specifically designed to obtain maximum ray density at the depth range between 100 and 300 km for teleseismic sources. In the period from 1998 August to 1999 May a total number of 1356 local, regional and teleseismic events was recorded. The data set will be used for multidisciplinary seismic tomography as well as anisotropy and receiver function studies (Bock *et al.* 2001).

3 3-D CRUSTAL MODEL: METHODOLOGY

We want to calculate accurately wave front distortions and traveltime effects of 3-D crustal structure on incoming teleseismic waves. Therefore, a proper parametrization of the crustal model has to include the causative crustal features, e.g. sedimentary basins, Moho topography and lateral variations in average velocity.

CSS methods are used to derive 3-D models of the crust. Reliability and precision of the CSS information depends on the observed data quality, interpretation methods and orientation of 2-D profiles with respect to 3-D structure. The reliability and error assessment of the various published CSS information collected over time is based on a weighting scheme that expresses the level of confidence of each individual seismic structure (Kissling 1993; Waldhauser *et al.* 1998). The degree of observation confidence is then transformed into an error estimate by computing the corresponding Fresnel volumes (Kissling *et al.* 1997). These error estimates are used in the interpolation of the profile data to produce a representative continuous crustal model. Other geophysical information, e.g. gravity data could be used in principle, but it would require several additional assumptions that could bias the simplicity and robustness of the crustal model and for that reason, we preferred not to include it in our model.

A detailed description of the methodology for the construction of the 3-D crustal model can be found in Waldhauser (1996) and Waldhauser *et al.* (1998). The construction as described by Waldhauser *et al.* (1998) and Arlitt *et al.* (1999) is performed in two steps. First, the Moho interface and topography is constructed and secondly the 3-D velocity structure is calculated. In the case of SVEKALAPKO, an anomalous high-velocity lower crust (Korja *et al.* 1993) demands an additional step.

In most regions, the crust–mantle boundary is represented by a sharp increase in seismic velocities and can easily be recognized by CSS methods. In refraction seismic experiments the Moho discontinuity is commonly observed as a wide-angle reflected (P_mP) and a refracted (P_n) phase. The corresponding reflector location and depth are the primary data to fix the crust–mantle boundary in a laterally extended model.

With sources and receivers on the same surface of the study volume, CSS experiments are 2-D methods applied to 3-D structure. Thus, proper locations of the reflectors must be found by migration

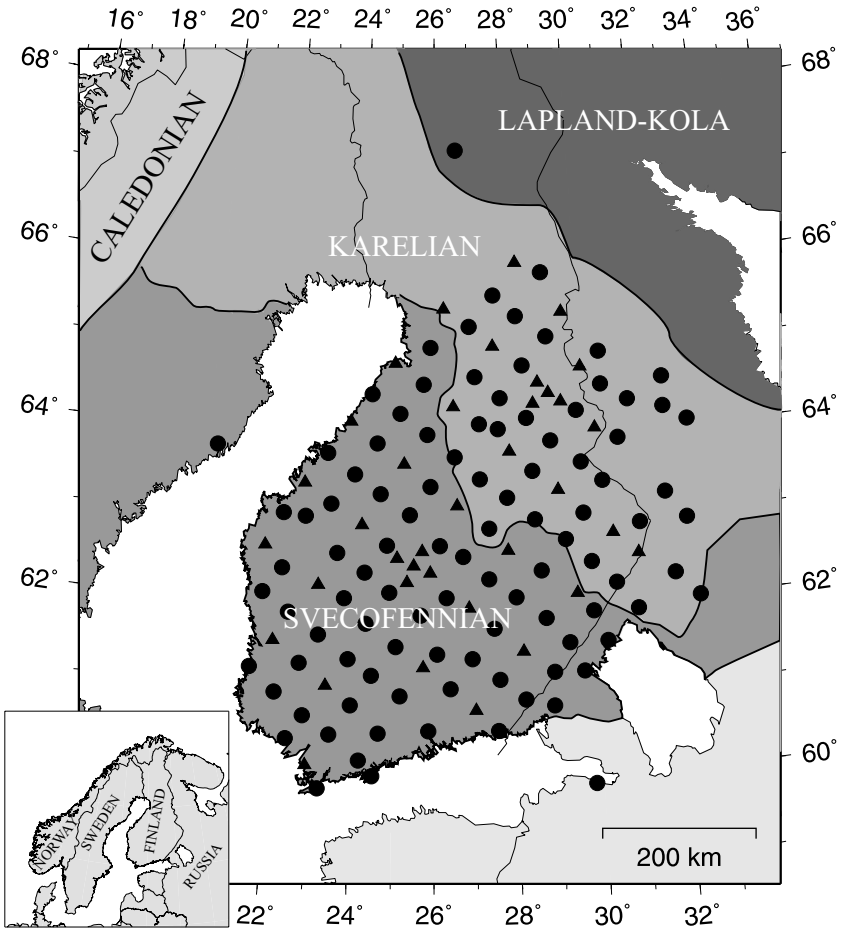

Figure 1. Tectonic map of the central part of the Baltic Shield and SVEKALAPKO seismic array (modified from Gorbatschev & Bogdanova 1993). The circles denote locations of short-period sensors and the triangles mark the position of the broad-band sensors.

before performing the final interpolation for the Moho interface. The correct spatial location of the reflectors is achieved through a 3-D migration scheme. 3-D migration can be separated into in-line migration and off-line migration. In-line migration is a common tool used in near-vertical reflection (e.g. Mayrand *et al.* 1987) and refraction experiments. Off-line migration refers to the fact that in a laterally varying structure the structural elements imaged along a profile may lie outside the vertical plane beneath the profile (Kissling *et al.* 1997).

After properly locating the reflectors, the final Moho interface is obtained by interpolation between reflectors (Waldhauser *et al.* 1998). The interpolation procedure follows the principle of simplicity (Kissling 1993): we seek the simplest (smoothest) Moho interface that fits all available CSS data within the previously assigned uncertainties. The derived Moho interface is then integrated in the Cartesian gridded model by discretization in 2 km steps in all three dimensions.

Interface depths (e.g. Moho) are not the only information extracted from CSS data. Velocity contrasts across interfaces and average velocities are also compiled and integrated in the model. Initially, the velocity–depth function at each model node assumes the values of an average 1-D crustal model compiled for the study region from all available data. After the integration of the calculated interfaces (e.g. Moho) into the 3-D model, all available local velocity information is attributed to the respective grid nodes. In order to accommodate the various types of velocity information, a velocity gradient between the surface and Moho is defined by default using two new parameters (Waldhauser 1996): the compensation depth and the compensation velocity. The variation of these two parameters provides a way to simulate different velocity gradients within the crust and still match the average velocities derived from the published CSS models.

4 3-D CRUSTAL MODEL FOR THE CENTRAL FENNOSCANDIAN SHIELD

The lithospheric structure of Fennoscandia has been studied in detail using several geophysical methods during the past decades. Among these studies, seismic experiments and especially CSS methods have played an important role. The first CSS experiments in the Baltic Shield were carried out in the late 1950s (Penttilä *et al.* 1960; Sellevoll & Penttilä 1964). Since then, a large number of CSS profiles for the crust have been acquired (Luosto 1997, and references therein). Recently, further detailed seismic velocity models for the Baltic Shield have been published: Malaska & Hyvonen (2000) derived a 3-D crustal model including the velocity distribution based on interpolation and smoothing of published 2-D seismic models. Yang *et al.* (2001) and Kremenetskaya *et al.* (2001) derived 1-D models for the lithosphere and upper mantle of the Baltic Shield derived from earthquake data.

We compiled the available CSS information for Fennoscandia from papers published in geophysical journals, from national

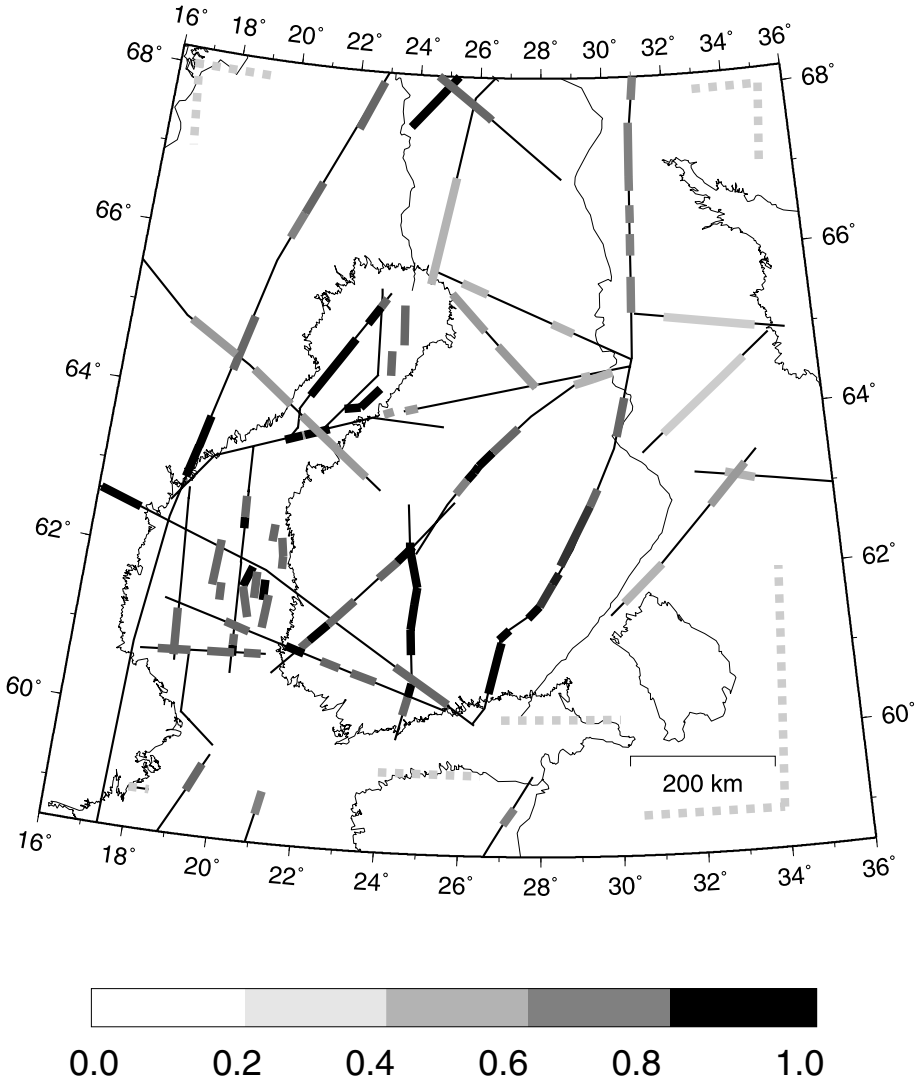

Figure 2. Location of the CSS experiments carried out in the study area (black lines). The thicker grey-shaded segments mark the reflectors used in the Moho interpolation. The grey-scale corresponds to the weight associated to each reflector (see text). The dashed lines are the synthetic reflectors.

reports and from personal communications. The completeness of this compilation (Fig. 2) is very important for the final crustal model because it determines the reliability of the lower lithosphere derived later on.

Moho interface

The central area of the Baltic Shield has been a traditional target of many CSS experiments. The seismic experiments are concentrated in the centre and the westernmost parts of the study area (Fig. 2). There are fewer seismic experiments in the easternmost part and these profiles are among the oldest in this area of the Baltic Shield (Luosto 1997). In order to stabilize the interpolation of the Moho interface additional synthetic reflectors (Fig. 2) were introduced in those model regions where no data were available. A uniform Moho depth of 42 km was assigned in these locations as a regionally representative value. The lowest weight in interpolation was used for the depth of these synthetic reflectors that are mainly situated at the corners of the study area (Fig. 2). These weights can be transformed into depth error estimates (Waldhauser *et al.* 1998), yielding a minimum Moho depth uncertainty of ± 2 km for the highest-quality reflectors and a Moho uncertainty of ± 10 km for the lowest-quality reflectors.

The final Moho interface (Fig. 3) is derived by interpolation of the 3-D migrated reflectors (Waldhauser *et al.* 1998). The most remarkable feature is a maximum crustal thickness of 64 km beneath the surface contact region between the Karelian and the Svecofennian blocks (Fig. 1). In general, the Svecofennian area shows a thicker crust than most of the Karelian or Lapland–Kola realm. A secondary maximum of crustal thickness is found beneath the western coast of Finland with a value of 56 km. A north-trending trough leads from the main maximum to the contact between the Karelian and the Lapland–Kola orogen with crustal thicknesses up to 52 km. From the northernmost edge of this narrow trough, a shallower broader trough (48 km on average) continues in a northwestern direction, which coincides with the location and orientation of the suture between the two tectonic units. The thinnest crust in the study region is observed in the surrounding terrains of the central Svecofennian Shield where the Moho is located at depths of between 38 and 42 km. Of course, these values are strongly influenced by the selected

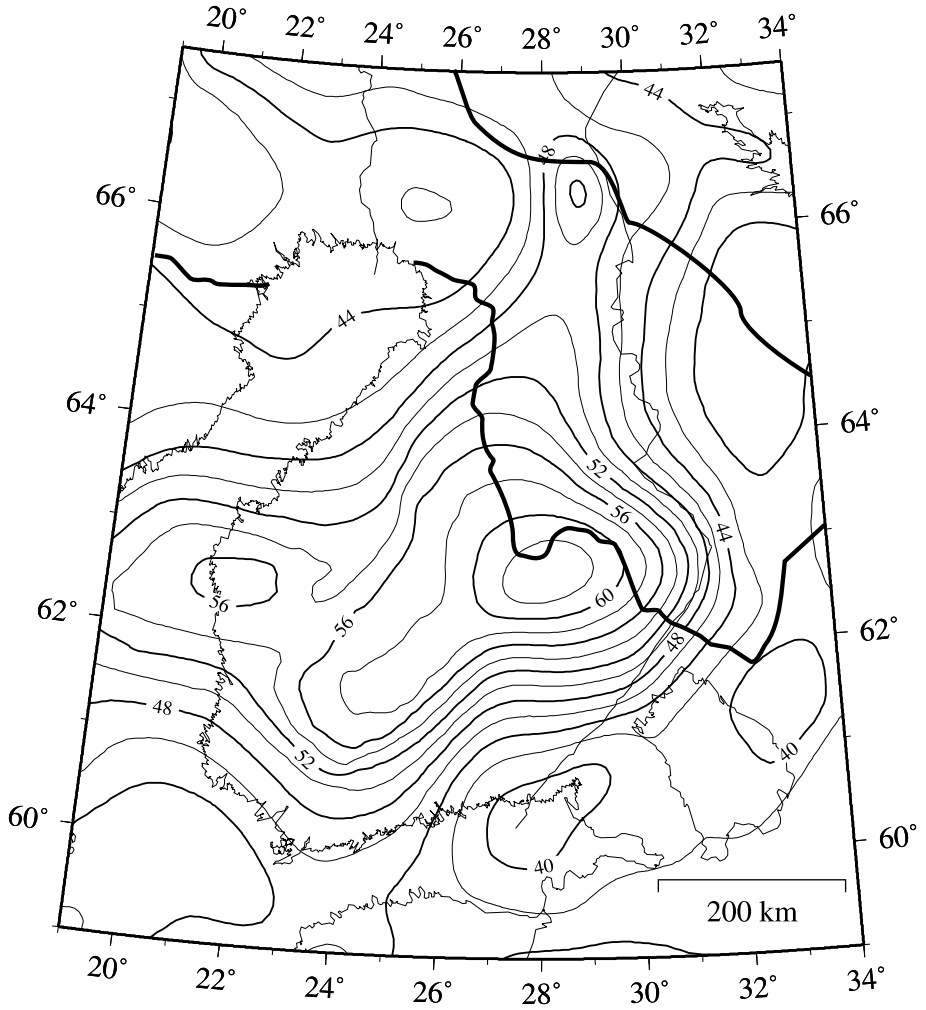

Figure 3. Contour map of the derived crustal thickness (in km) for the study area derived from interpolation of the 3-D migrated Moho reflectors and main tectonic regions (solid thick lines).

regional averaged model (42 km). The derived Moho interface is in good accordance with previous models (e.g. Luosto 1997, and references therein) owing to the coincident input data. The minor differences arising from different interpolation schemes used in either study are not significant.

High-velocity lower crust

Besides the variable thickness of the crust, another relevant feature of the SVEKALAPKO crustal model is the thickness of the lower crust with anomalously high velocities in some regions. In the Baltic Shield, this layer accounts for most of the crustal thickness variation. The anomalous high-velocity lower crustal layer demands special adjustments to the process of velocity modelling as outlined by Waldhauser *et al.* (1998) and Arlitt *et al.* (1999). In the modified procedure, the top of the lower crust is introduced in the 3-D model as a second reference interface in addition to the Moho. The top of the high-velocity lower crust under the central part of the Baltic Shield is defined as the depth at which the *P*-wave velocity reaches 7.0 km s^{-1} (Korja *et al.* 1993). In these regions of thicker crust, velocities of *P* waves up to 7.85 km s^{-1} are observed just above the Moho interface. These high velocities in the lower crust have a significant influence on the average crustal velocity. Korja *et al.* (1993) concluded that in some regions, the lower crust under the Baltic Shield shows petrophysical characteristics similar to those that can be found in mantle rocks. They suggest that this layer consists of a combination of mafic lower crust from the island arc crustal blocks with additions from a possible delamination of the post-collisional lithosphere.

P-wave velocity structure of the crust

In central Fennoscandia, two interfaces must be accounted for in the 3-D velocity model: the Moho and the upper limit of the lower crust. We assign a constant velocity of 8.3 km s^{-1} to the base of the model at 70 km (Fig. 4). This value is calculated by averaging the CSS velocities at that depth. At the surface, a constant value of 5.9 km s^{-1} is also chosen as an average value derived from the CSS experiments. The SVEKALAPKO study area is characterized by the lack of sediments at the surface.

Owing to the vertical differentiation, the velocity interpolation is achieved in two steps. Two velocity gradients are defined, the first between the surface and the top of the high-velocity lower crust and the second between the upper limit of the high-velocity lower crust and the Moho. When these two velocity gradients match the average crustal velocity field, an interpolation is applied among the

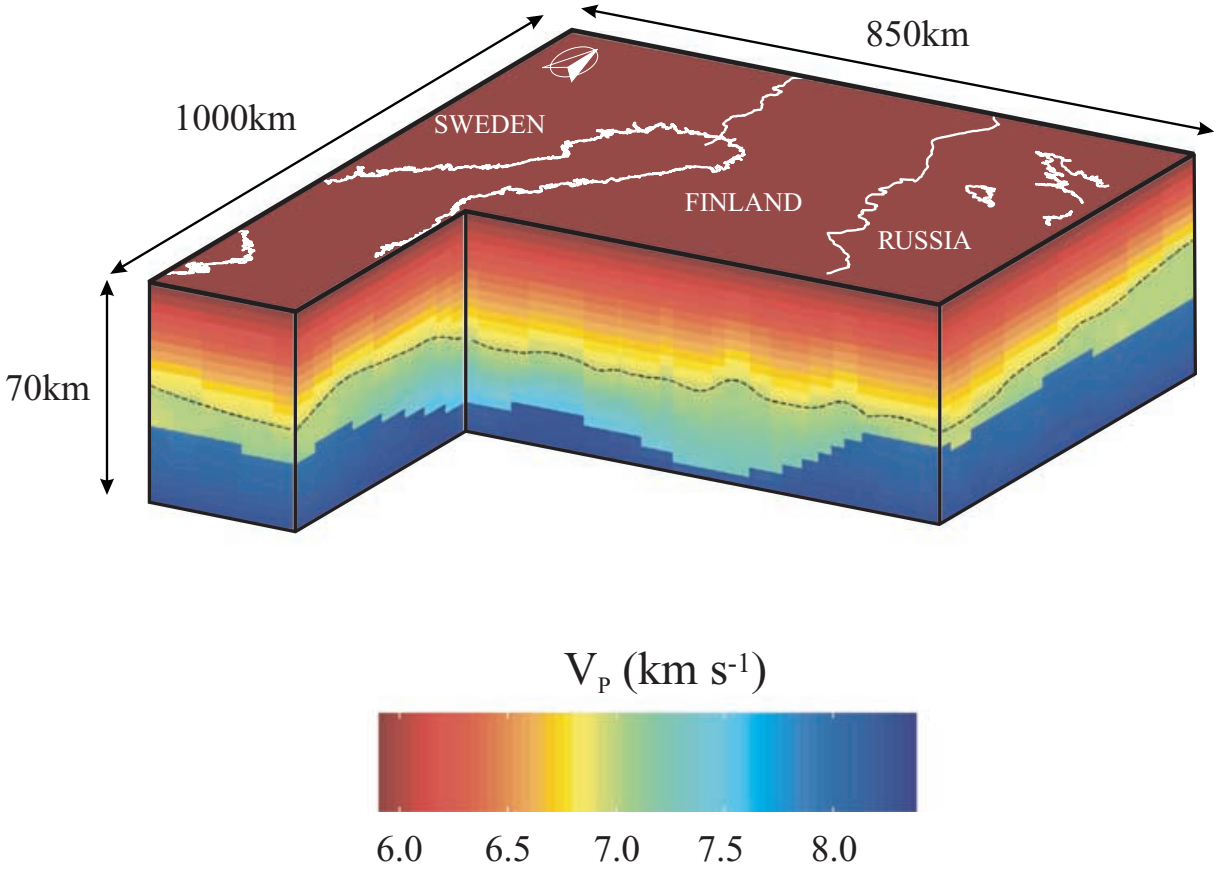

Figure 4. Crustal block with cross-sections of *P*-velocity distribution of the 3-D crustal model under the SVEKALAPKO study area. The dashed black line shows the upper limit of the anomolous high-velocity lower crust adapted from Korja *et al.* (1993).

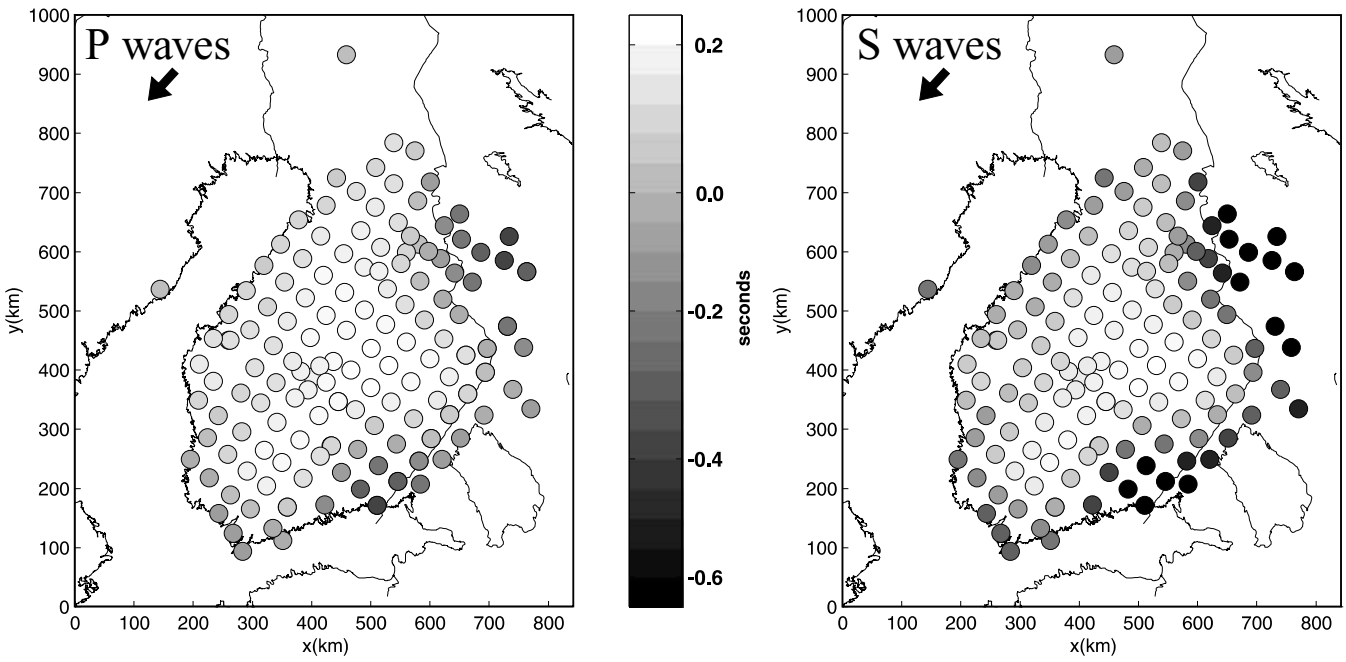

Figure 5. Traveltime differences for one event between the derived 3-D crustal model (left-hand panel for *P* waves and right-hand panel for *S* waves) and the global reference model IASP91. The black arrow shows the azimuth of the incoming wave front.

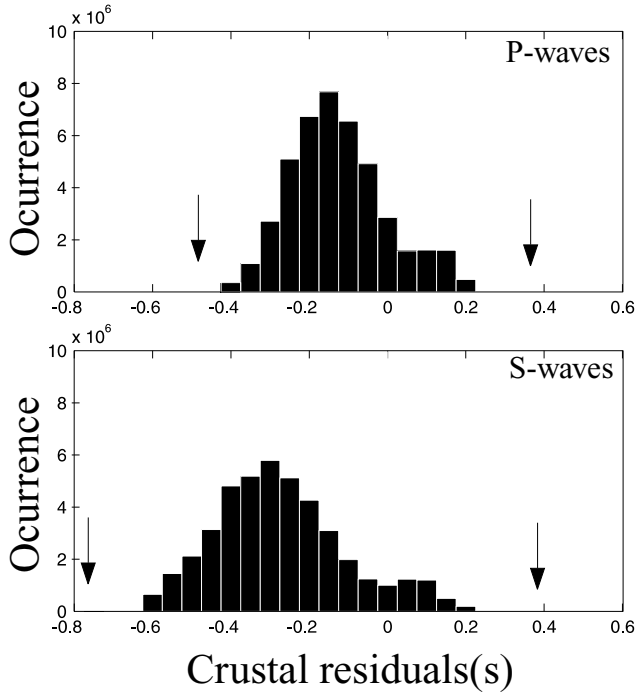

Figure 6. Histograms of the calculated traveltime differences between the 3-D crustal model and the global reference model IASP91 (upper figure for *P* waves and lower figure for *S* waves). The arrows mark the maximum and minimum differences in each case.

different reflector locations to establish the 3-D velocity field. Fig. 4 shows a perspective view of two cross-sections through the final 3-D crustal model with crustal depth and *P*-wave velocity distribution. The main features of the crustal model are clearly visible (Fig. 4), e.g. the maximum crustal thickness of 64 km and the high-velocity lower crust (V_p > 7.0 km s^{-1}), which accounts for most of the anomalous crustal thickness.

Shear wave velocity model

Ideally, an analogous process would lead to a model for *S*-wave velocities. However, there are fewer (and lower-quality) *S*-wave Moho reflections. For that reason, the *S* model is derived from the *P* model. The Moho interface is taken from the *P*-wave modelling and the *S*-wave velocities are derived by applying V_P/V_S ratios representative for the Baltic Shield as derived by Luosto (1997) and Korsman *et al.* (1999) with values of 1.71, 1.76 and 1.78 for the upper crust, lower crust and upper mantle, respectively.

5 TELESEISMIC TRAVELTIME EFFECTS OF CRUSTAL STRUCTURE

The purpose of establishing the described 3-D crustal model is to calculate traveltime residuals for incoming teleseismic waves, since crustal effects cannot be derived by teleseismic tomography alone. Traveltimes through the compiled 3-D crustal model are determined with the 3-D finite-difference algorithm of Hole & Zelt (1995). To obtain entry points and arrival times for teleseismic waves at the

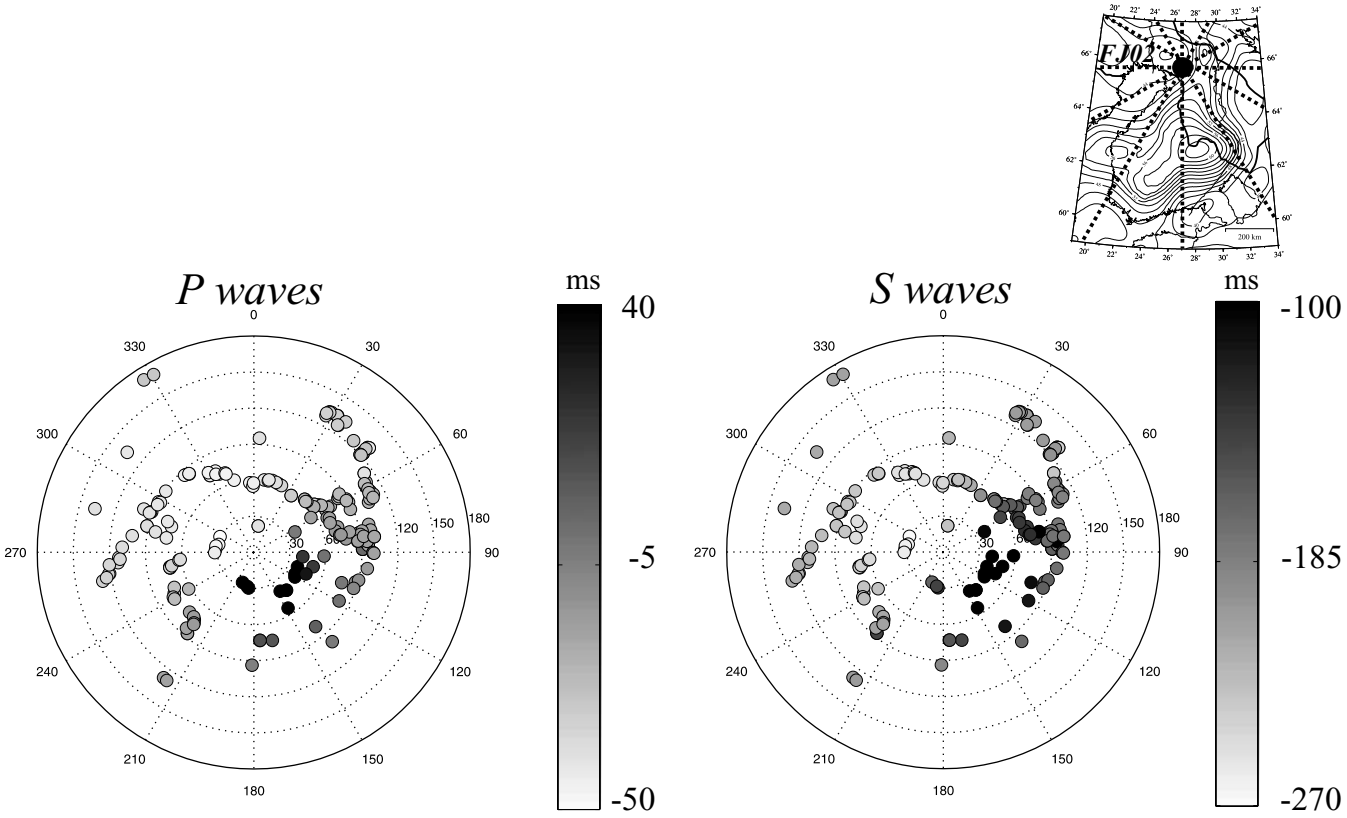

Figure 7. Azimuthal and distance variation of the calculated traveltime delays (left-hand panel for *P* waves and right-hand panel for *S* waves) for station FJ02 (see the inset map).

bottom of the crustal model we employ the spherical 1-D reference model IASP91 (Kennett & Engdahl 1991).

Fig. 5 shows the traveltime differences between the 3-D crustal model (both *P* and *S*) and the 1-D reference IASP91 model for an event from Japan arriving at the SVEKALAPKO array. The stations situated in the centre of the array show the largest positive delays with 0.22 s for the *P*- and 0.24 s for the *S* model. The area with positive delays coincides with thicker crust, although the retarding effect of the crust is significantly reduced by the presence of the fast lower crust (Fig. 4). If the anomalous high-velocity lower crust were not taken into account, the positive delays in the central part of the array would in general double. Early arrivals are obtained in the surrounding areas, with minimum values of −0.43 s for the *P* model and −0.62 s for the *S* model. At first glance this result is surprising, since the average crustal thickness here is 42 km (7 km thicker than IASP91) and therefore, larger residuals in this region could be expected compared with IASP91. The reason for the early arrivals, however, is the presence of high average velocities in the crust, and particularly, the high-velocity lower crust. This layer increases the average crustal velocity to values close to 6.4 km s^{-1} (IASP91 has an average crustal velocity of 6.1 km s^{-1}).

Fig. 6 documents the traveltime differences calculated at each model surface gridpoint for a set of 202 selected and azimuthally different teleseismic events recorded during the SVEKALAPKO experiment. The delays associated with the 3-D *P* model relative to IASP91 have a distribution centred at −0.15 s with maximum and minimum delays of 0.37 and −0.49 s, respectively. The *S*-wave delay distribution is centred at −0.30 s with a maximum value of 0.38 s and a minimum delay of −0.76 s. Both distributions show a similar pattern. This is an expected result since the *S* model is derived from the *P* model. In both distributions a secondary maximum can be observed between 0.00 and 0.20 s. This population of positive delays is caused by the points that lie in the area with thickest crust.

Variations in the calculated delays are expected at a specific surface point depending on the azimuthal distribution of the source (Fig. 7). Azimuthally, the larger delays correspond to those events incoming from the SSE. There are also variations with the angle of incidence, i.e. the larger the epicentral distance is the smaller the azimuthal variation becomes. When the incident angle approaches 90°, the difference in the ray path through the crust decreases and the variation is smaller.

6 HIGH-RESOLUTION REGIONAL TELESEISMIC TOMOGRAPHY IN FENNOSCANDIA

Synthetic tests are of paramount importance in any inversion since they provide quantitative information concerning the resolution of the data and they can help to distinguish real features from artefacts (Kissling *et al.* 2001). We design a synthetic mantle structure (Fig. 8) composed of two anomalies: a positive anomaly of 1.5 per cent between 100 and 200 km depth and a negative anomaly of −3.0 per cent between 200 and 300 km depth. We then calculate synthetic traveltimes including the IASP91 crust for those 5126 rays that were observed during the SVEKALAPKO body wave tomography experiment (Fig. 9). Note that these synthetic traveltimes are comparable in magnitude with those observed in the real data. Adding to these upper-mantle traveltimes the effects of the SVEKALAPKO 3-D crustal model and a Gaussian distributed error of $\sigma = 0.1$ s, results in a realistic synthetic data set ready for inversion. All inversion tests have been repeated with variable input parameters (grid spacing, damping, number of iterations) until optimal values were found. The analysis of the influence of each of these parameters on the inversion is beyond the scope of this work. Only the influence of the crustal features is discussed. The inversion grid consists of 50 × 50 km^2 blocks. The vertical dimension of the blocks varies with depth from 20 km in the crust and increases to 50 km at a depth of 450 km (Fig. 8).

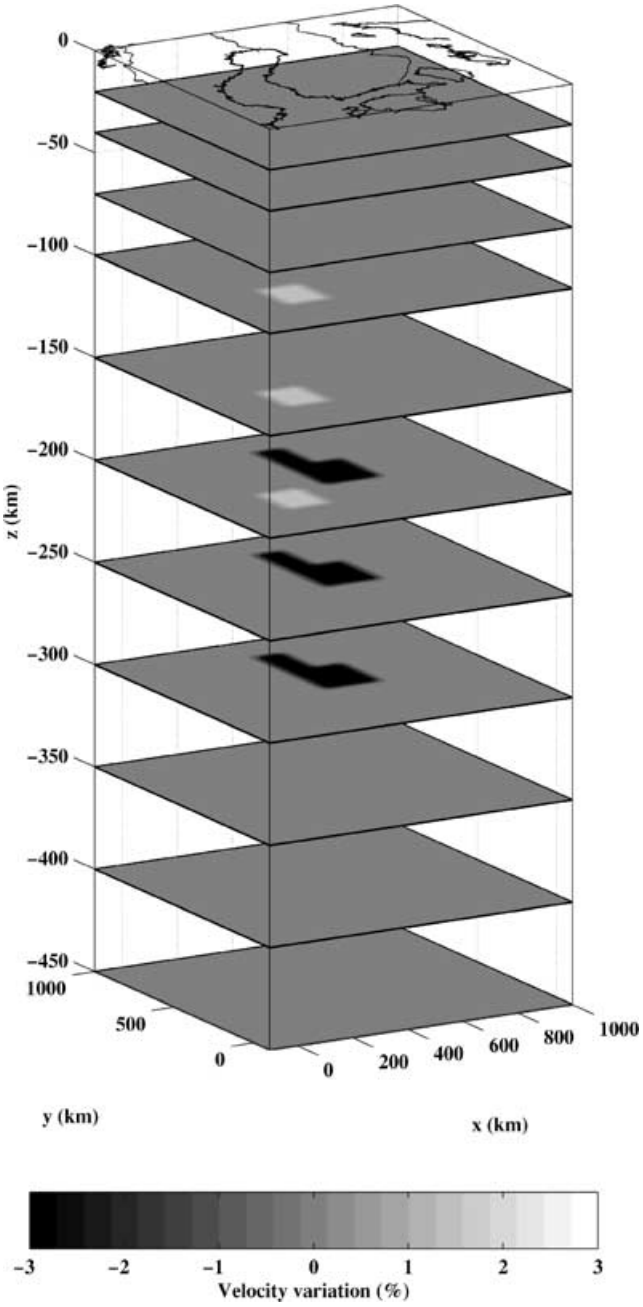

Figure 8. Synthetic mantle structure used for the inversion test. The vertical exaggeration is 6:1.

To assess the influence of the crustal correction on the resolution of the upper-mantle structure, we have designed two inversion tests. First, the synthetic data set is inverted: (1) for crustal and mantle structure combined and (2) for mantle structure only after correction for crustal effects. Option (1) is a commonly used approach based on the assumption that if crustal anomalies are present, the

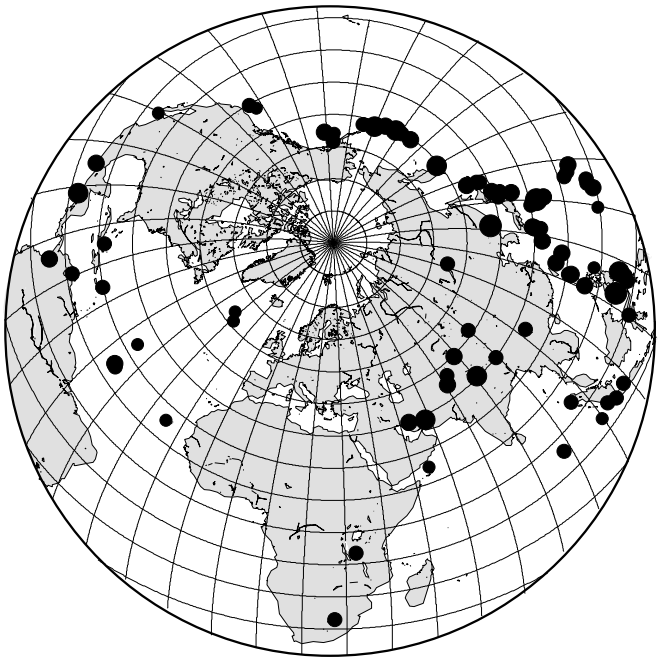

Figure 9. Distribution of teleseismic events recorded at the SVEKALAPKO array used for the construction of the synthetic traveltime data set.

crustal effects are less likely to produce artefacts at mantle depths if the crustal cells are also inverted for, i.e. if they are allowed to be adjusted during non-linear inversion.

The results of the first test are displayed in Fig. 10. On the left-hand side, the results for option (1) are shown. The recovered structure is highly influenced by the crust in the upper layers of the mantle. The anomaly pattern at 70, 100 and 150 km depth can be clearly correlated with the crustal anomalies (Fig. 5). The crustal residuals completely mask the presence of the positive anomaly. Yet, the negative anomaly starting at 200 km can be fairly well recovered, due probably to its larger depth and amplitude. Note that the larger horizontal sensitivity is caused by the subvertical incidence of the incoming rays. The horizontal extension of the negative anomaly is well outlined, showing a sharp contrast with the surrounding medium. The vertical resolution is smaller and the anomaly is smeared to the neighbouring layers above and below. Some weaker anomalies appear in the deepest layers.

Applying option (2) of the first test (Fig. 10b), the crustal layers are fixed to 70 km depth by model IASP91 and the synthetic traveltimes are crust-corrected. The main differences are observed in the layers lying immediately beneath the crust. The leakage from the crust has disappeared and the positive anomaly is now clearly recovered. The number of anomalies in the rest of the layers decreases and the contrast of the introduced anomalies is now clearer at all depth levels. From this test it is clear that resolution at upper-mantle levels improves significantly if 3-D crustal corrections are applied. It is important to note here that any mismatch between the real crustal structure and the modelled one will be projected into the underlying layers.

The second test studies the direct effects of 3-D crustal structure on non-linear inversion results for the upper mantle. This corresponds to a synthetic data test where a laterally uniform mantle structure is overlain by the 3-D crustal model of Fennoscandia. The calculated crustal traveltime residuals are inverted, allowing all nodes from the surface to a depth of 450 km to be adjusted freely. In this way, we evaluate whether the inversion process correctly identifies these residuals as being produced by the shallowest layers (crust). This test further serves the purpose of identifying the artefacts caused by crustal structure in the uppermost mantle that may not be defined otherwise because of the non-linearity of the problem. With this second test (Fig. 11) the crustal effect in the recovered mantle image can be clearly observed. The results document that the

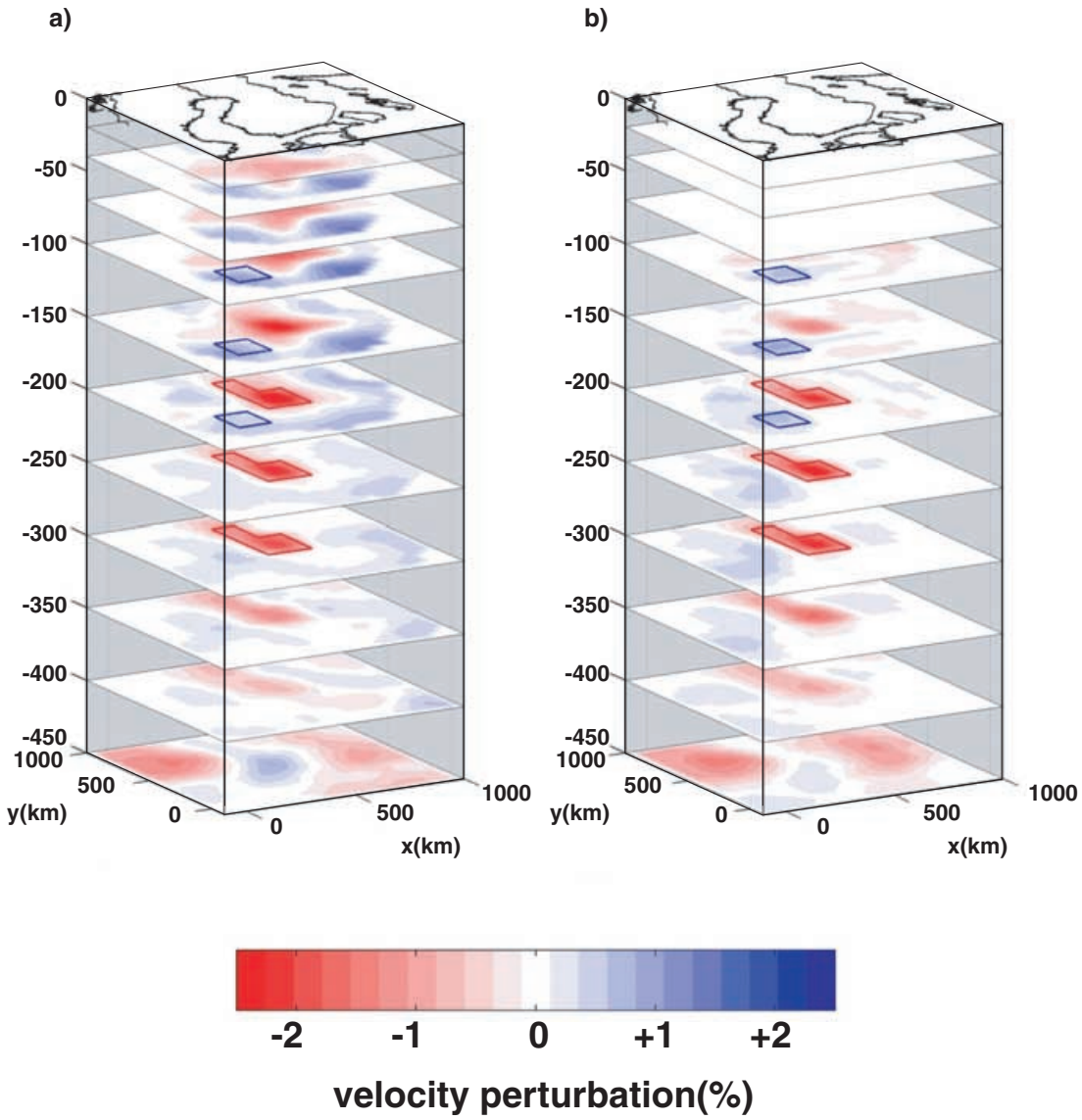

Figure 10. Inversion results of synthetic data documenting the effects of the 3-D crustal corrections on the structure of the upper-mantle. Blue and red frames are the locations of the input velocity anomalies. (a) Recovered *P*-wave velocity variations after inverting the traveltime residuals from the 3-D crust and the synthetic velocity anomalies. The crustal nodes are floating. (b) Recovered *P*-wave velocity variations after inverting the crustal-corrected traveltime residuals produced by the synthetic anomalies. The crustal nodes are fixed. Vertical exaggeration in both figures is 6:1. In all cases, the results after the first iteration are shown.

inversion does not constrain the crustal anomalies to the shallowest layers. Rather, we note a strong leakage of crustal effects down to 200 km. Beneath this depth, the crustal effects decrease but they do not disappear and can still be found at 450 km depth.

7 DISCUSSION

We have constructed a 3-D crustal model for the central part of the Baltic Shield following the principle of simplicity as defined by Kissling *et al.* (1997). The model derived by CSS data has a maximum thickness of 64 km under the surface contact between the Karelia and the Svecofennian blocks. The model also includes clear velocity contrasts at the Moho, average crustal velocities and the presence of an anomalous high-velocity lower crust. The integration of these features in the crustal model leads to a more accurate and complete assessment of the crustal contribution to the teleseismic traveltimes and their lateral variations through it. Despite the extraordinary structural variations of the crust beneath the SVEKALAPKO array, the calculated *P*-wave teleseismic traveltime residuals do not deviate by more than ± 0.4 s from those traveltimes obtained using the 1-D reference model IASP91. This is owing to the presence of the high-velocity lower crust, which accounts for most of the crustal thickness variations. Similar results were found by Wilde-Piórko *et al.* (1999). They observed larger time delays only for stations located on the Palaeozoic platform in northern Poland outside the Precambrian platform. Arlitt *et al.* (1999) calculated anomalies of $+0.4$ s for the southernmost part of the Baltic Shield. The main difference between their model for the Baltic Shield and the one presented in this work is the presence of the high-velocity lower crust that compensates for the positive delays owing to the thickening of the crust. Despite the smooth pattern and small amplitude of the variations of crustal traveltime residuals calculated for the Baltic

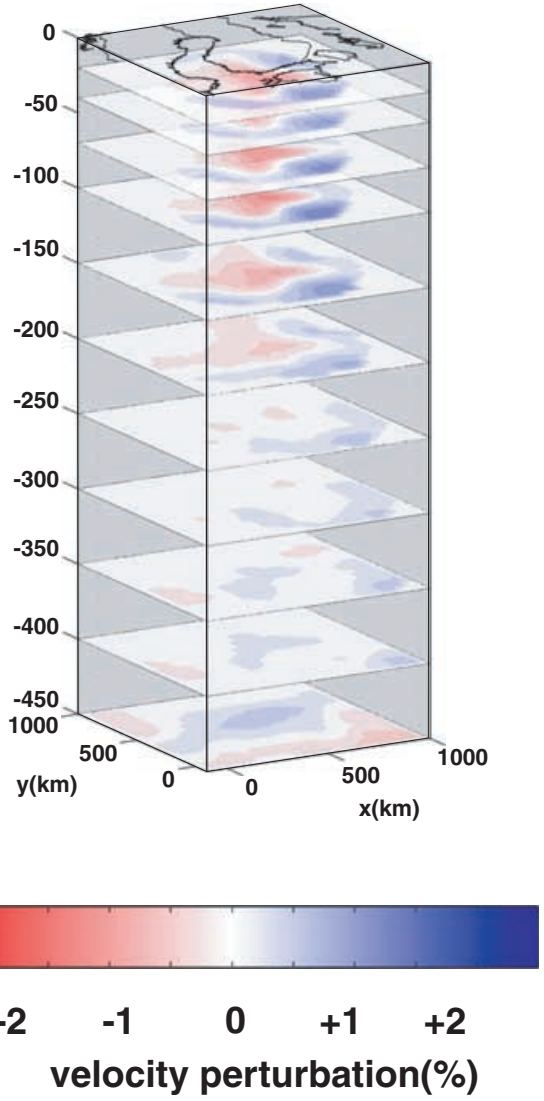

Figure 11. Recovered *P*-wave velocity variations after inverting only the traveltime residuals generated by the 3-D crust. All nodes are floating. The vertical exaggeration is 6:1.

Shield, these variations play an important and unexpected role in the subsequent inversion as documented by our synthetic tests. Assuming that the CSS input data for the crustal structure are sufficient to establish a representative model, the calculated crustal residuals permit a precise correction of the observed teleseismic traveltimes at the SVEKALAPKO array. However, it is important to note that the crustal corrections are not error-free. Rather, they represent the best possible approximation that can be derived from available data.

As a final test, we compare our crustal correction method with other approaches (Fig. 12). In Fig. 12(a), we display the average crustal velocity variations at 40 km depth for our 3-D crustal model. The average velocity is calculated for the depth range between 30 and 50 km, corresponding to the top and bottom of the inversion cell at 40 km depth. At this depth level the volume average velocity is clearly influenced by the Moho topography and the anomalous high-velocity lower crust (compare with Fig. 3). After calculating the average velocities, the mean value is removed in order to obtain a zero mean distribution as obtained in the inversion result. By this kind of display the features of the *a priori* 3-D crustal model may be compared with the recovered structure resulting from inversion of the corresponding crustal traveltime effects. Then the calculated traveltime residuals owing to the 3-D crustal model alone (i.e. the homogenous mantle) are inverted, allowing all the model space to absorb the anomalies (Fig. 11). Fig. 12(b) shows the results for the depth level at 40 km depth. The recovered anomalies are highly damped because of the very strong leakage of the crustal structure into the lithosphere and upper mantle (Fig. 11). The inversion results of the 'stripping method' proposed by Takauchi & Evans (1995) for the same depth level are shown in Fig. 12(c). In this case, the data used in the inversion are real, as opposed to the synthetic data set used in Figs 12(a) and (b). The results clearly document the insufficient cross-firing of the rays within the crust. The overall pattern of the true crustal anomalies (Fig. 12a) is lost while several other features are observed, probably arising from lower lithospheric and upper-mantle contamination. The amplitude of the recovered anomalies is similar to the 3-D crustal model; however, this model is prone to producing significant artefacts. Finally, in Fig. 12(d) the inversion results are shown at 40 km depth for the observed traveltime residuals without crustal corrections. In this case all the nodes of the model space are allowed to float. The result has similar characteristics to the previous one, except for the smaller amplitude of the anomalies. This fact results from the same reasons as mentioned in Fig. 12(b). This documents the advantage of the method proposed here to account for crustal structure.

8 CONCLUSIONS

Proper correction for lateral variations of crustal structure is another important aspect for teleseismic tomography studies of the upper mantle. We have demonstrated for the Baltic Shield the importance of these corrections to observed teleseismic traveltimes prior to their inversion for upper-mantle structure. According to the results of our second test (inversion of only crustal residuals), we conclude that teleseismic tomography cannot satisfactorily resolve 3-D crustal structure despite the fact that incoming teleseismic wave fronts are severely affected by the uppermost crustal structure. More reliable images of the uppermost mantle are obtained by removing the strong downward leakage produced by the crust. In regions with larger crustal anomalies, e.g. active tectonic margins with sedimentary basins or strong velocity variations in the crust, an even larger influence of the crust on the underlying structure is expected. Therefore, appropriate 3-D crustal corrections generally appear to be very important for high-resolution teleseismic tomography of the upper mantle.

ACKNOWLEDGMENTS

We would like to thank J. Yliniemi, N. Sharov and N. Pavlenkova for providing additional seismic profiles to derive the crustal model. We also thank G. Bock, R. Roberts and one anonymous reviewer for their useful suggestions. This is contribution number 1256 from the Institute of Geophysics, ETH Zurich. The following institutions participate in the SVEKALAPKO project: Universities of Oulu, Helsinki, Uppsala, Grenoble, Strasbourg, Stuttgart, St Petersburg, Kola Science Center, Institute of Physics of the Earth Moscow, ETH Zurich, GFZ Potsdam, Geophysical Institute of CAS Prague and Spezgeofisika MNR Moscow. The SVEKALAPKO project has been supported by national science funding agencies in Finland, France, Sweden and Switzerland, by the Institute of Geophysics of the Polish Academy of Sciences, by GeoForschungsZentrum Potsdam (GFZ),

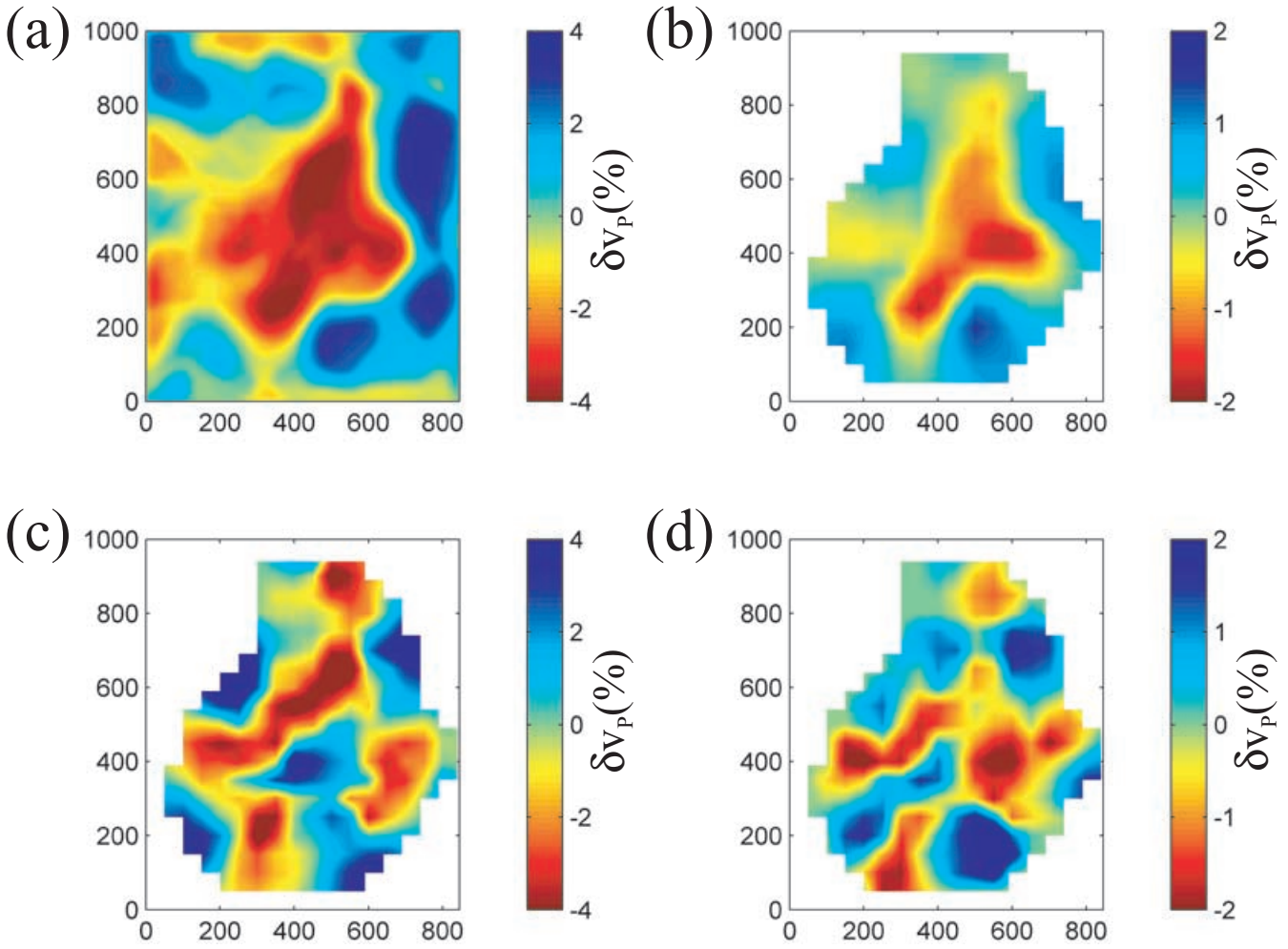

Figure 12. (a) Relative *P*-velocity variation of the SVEKALAPKO 3-D crustal model at 40 km depth. The velocities are averaged between 30 and 50 km depth. (b) Recovered structure at 40 km depth after inverting the traveltime residuals generated by the 3-D crustal model only (compare with section at 40 km depth in Fig. 10). (c) Recovered structure at 40 km depth after inverting the observed traveltime residuals and forcing the inversion to allocate the maximum of anomalies into the shallower levels (Takauchi & Evans 1995). (d) Recovered structure at 40 km depth after inverting the observed traveltime residuals and letting the inversion to allocate the anomalies all over the model space. All colour scales represent *P*-velocity variations as a percentage.

by the GFZ Geophysical Instrument Pool and by an EU INTAS grant. Thanks are due to the European Science Foundation ESF for supporting several workshops of the SVEKALAPKO groups in St Petersburg and Lammi, Finland through their international programme EUROPROBE.

The SVEKALAPKO seismic tomography working group consists of: U. Achauer, A. Alinaghi, J. Ansorge, G. Bock, M. Bruneton, W. Friederich, M. Grad, P. Heikkinen, S.-E. Hjelt, T. Hyvonen, J.-P. Ikonen, E. Kissling, K. Komminaho, A. Korja, E. Kozlovskaya, H. Paulssen, N. Pavlenkova, H. Pedersen, J. Plomerova, T. Raita, R. G. Roberts, S. Sandoval, I. A. Sanina, N. Sharov, H. Shomali, E. Wielandt, K. Wylegalla and J. Yliniemi.

REFERENCES

Aki, K., Christofferson, A. & Husebye, E., 1977. Determination of the three-dimensional seismic structure of the lithosphere, *J. geophys. Res.,* **82,** 277–296.

Arlitt, R., Kissling, E., Ansorge, J. & TOR Working Group, 1999. Three-dimensional crustal structure beneath the TOR array and effects on teleseismic wavefronts, *Tectonophysics,* **314,** 309–319.

Bijwaard, H., Spakman, W. & Engdahl, E., 1998. Closing the gap between regional and global travel time tomography, *J. geophys. Res.,* **103,** 30 055–30 078.

Blundell, D., Freeman, R. & Mueller, S., eds, 1992. *A Continent Revealed, the European Geotraverse,* p. 275, Cambridge University Press.

Bock, G. & the SVEKALAPKO Seismic Tomography Working Group, 2001. Seismic probing of Archean and proterozoic lithosphere in Fennoscandia, *EOS, Trans. Am. geophys. Un.,* **82,** 621,628–629.

Dziewonski, A.M. & Anderson, D.L., 1983. Travel-times and station corrections for *P*-waves at teleseismic distances, *J. geophys. Res.,* **88,** 3295–3314.

Engdahl, E., van der Hilst, R. & Buland, R., 1998. Global teleseismic earthquake relocation with improved travel times and procedures for depth determination, *Bull. seism. Soc. Am.,* **88,** 722–743.

Evans, J.R. & Achauer, U., 1993. Teleseismic velocity tomography using the ACH method: theory and application to continental scale studies, in *Seismic Tomography,* pp. 319–360, eds Iyer, H.M. & Hirahara, K., Chapman and Hall, London.

Gee, D. & Zeyen, H., eds, 1996. *EUROPROBE 1996—Lithosphere Dynamics: Origin and Evolution of Continents,* EUROPROBE Secretariate, Uppsala University, p. 138.

Giese, P., Prodehl, C. & Stein, A., eds, 1976. *Explosion Seismology in Central Europe: Data and Results,* Springer, Berlin, p. 429.

Gorbatschev, R. & Bogdanova, S., 1993. Frontiers in the Baltic Shield, *Precambrian Res.,* **64,** 3–21.

Gutenberg, B., 1959. *Physics of the Earth's Interior, Int. Geophysics Series,* vol. I, p. 240, New York: Academic Press.

Hole, J.A. & Zelt, B.C., 1995. 3-D finite-difference reflection travel times, *Geophys. J. Int.,* **121,** 427–434.

Julian, B., Evans, J., Pritchard, M. & Foulger, G., 2000. A geometrical error in some computer programs based on the Aki–Christofferson–Husebye (ACH) method of teleseismic tomography, *Bull. seism. Soc. Am.,* **90,** 1554–1558.

Kennett, B. & Engdahl, E., 1991. Travel times for global earthquake location and phase identification, *Geophys. J. Int.,* **105,** 429–465.

Kissling, E., 1993. Deep structure of the Alps—what do we really know?, *Phys. Earth planet. Inter.,* **79,** 87–112.

Kissling, E., Ansorge, J. & Baumann, M., 1997. Methodological considerations of 3-D crustal structure modelling by 2-D seismic methods, in *Deep Structure of the Swiss Alps,* pp. 31–38, eds Heitzmann, P., Lehner, P., Mueller, S., Pfiffner, A. & Steck, A., Birkhäuser, Basel.

Kissling, E., Husen, S. & Haslinger, F., 2001. Model parameterization in seismic tomography: a choice of consequence for the solution quality, *Phys. Earth planet. Inter.,* **123,** 89–101.

Korja, A., Korja, T., Luosto, U. & Heikkinen, P., 1993. Seismic and geoelectric evidence for collisional and extensional events in the Baltic Shield—implications for Precambrian crustal evolution, *Tectonophysics,* **219,** 129–152.

Korsman, K., Korja, T., Pajunen, M., Virransalo, P. & the GGT/SVEKA Working Group, 1999. The GGT/SVEKA transect: structure and evolution of the continental crust in the Paleoproterozoic Svecofennian Orogen in Finland, *Int. Geol. Rev.,* **41,** 287–333.

Kremenetskaya, E., Asming, V. & Ringdal, F., 2001. Seismic location calibration of the European Arctic, *Pure appl. Geophys.,* **158,** 117–128.

Luosto, U., 1997. Structure of the Earth's Crust in Fennoscandia as revealed from refraction and wide-angle reflection studies, in *The Lithosphere in Finland—a Geophysical Perspective,* pp. 3–16, ed. Pesonen, J., Geophysical Society of Finland, Helsinki.

Malaska, J. & Hyvonen, T., 2000. Velocity modelling of the lithosphere beneath south Finland, *Phys. Earth planet. Inter.,* **122,** 103–114.

Masson, F. & Trampert, J., 1997. On ACH, or how reliable is regional teleseismic delay time tomography?, *Phys. Earth planet. Inter.,* **102,** 21–32.

Mayrand, L.J., Green, A.G. & Milkereit, B., 1987. A quantitative approach to bedrock velocity resolution and presision: the LITHOPROBE Vancouver Island Experiment, *J. geophys. Res.,* **92,** 4837–4845.

Penttilä, E., Karras, M., Nurmia, M., Siivola, A. & Vesanen, A., 1960. Report on the 1959 explosion seismic investigation in Southern Finland, University of Helsinki, Publications in Seismology, Helsinki.

Rohm, A., Bijwaard, H., Spakman, W. & Trampert, J., 2000. Effects of arrival time errors on travel time tomography, *Geophys. J. Int.,* **142,** 270–276.

Sandoval, S., Kissling, E., Ansorge, J. & the SVEKALAPKO Seismic Tomography Working Group, High-Resolution body wave tomography beneath the SVEKALAPKO array: II. Anomalous Upper Mantle Structure Beneath the Central Baltic Shield, *Geophys. J. Int.,* submitted.

Sellevoll, M.A. & Penttilä, E., 1964. Seismic refraction measurements of crustal structure in Northern Scandinavia, *Årbok Univ. Bergen, Mat.-Naturv,* **9**, 10s.

Takauchi, Y. & Evans, J., 1995. Teleseismic tomography of the Loma Prieta aerthquake region, California: implications for strain partitioning, *Geophys. Res. Lett.,* **22,** 2203–2206.

Thurber, C.H. & Kissling, E., 2000. Advances in travel time calculations for three-dimensional structures, in, *Advances in Seismic Event Location*, p. 29, eds Thurber, C.H. & Rabinowitz, N., Chapter 4, Kluwer, Dordrecht.

VandeCar, C.J., James, D.E. & Assumpcao, M., 1995. Seismic evidence for a fossil mantle plume beneath South America and implications for plate driving forces, *Nature,* **378,** 25–31.

Waldhauser, F., 1996. A parameterized three-dimensional Alpine crustal model and its application to teleseismic wavefront scattering, *PhD thesis,* no 11940, ETH Zurich, Switzerland.

Waldhauser, F., Kissling, E., Ansorge, J. & Mueller, S., 1998. 3-D interface modelling with 2-D seismic data: the Alpine crust–mantle boundary, *Geophys. J. Int.,* **135,** 264–278.

Wilde-Piórko, M., Grad, M. & POLONAISE Working Group, 1999. Regional and teleseismic events recorded across the TESZ during POLONAISE'97, *Tectonophysics,* **314,** 161–174.

Yang, X., Bondar, I., McLaughlin, K. & North, R., 2001. Source specific station corrections for regional phases at Fennoscandian stations, *Pure appl. Geophys.,* **158,** 35–57.